ARTICLE

Role of Bridge-bonded Formate in Formic Acid Dehydration to CO at Pt Electrode: Electrochemial *in-situ* Infrared Spectroscopic Study

Zun-biao Zhang, Jie Xu, Jing Kang, Yan-xia Chen*

Hefei National Laboratory for Physical Science at Microscale and Department of Chemical Physics, University of Science and Technology of China, Hefei 230026, China

(Dated: Received on April 11, 2013; Accepted on May 16, 2013)

Formic acid (HCOOH) decomposition at Pt film electrode has been studied by electrochemical *in situ* FTIR spectroscopy under attenuated-total-reflection configuration, in order to clarify whether bridge-bonded formate ($HCOO_b$) is the reactive intermediate for CO_{ad} formation from HCOOH molecules. When switching from HCOOH-free solution to HCOOH-containing solution at constant potential (E=0.4 V *vs.* RHE), we found that immediately upon solution switch CO_{ad} formation rate is the highest, while surface coverage of formate is zero, then after CO_{ad} formation rate decreases, while formate coverage reaches a steady state coverage quickly within ca. 1 s. Potential step experiment from E=0.75 V to 0.35 V, reveals that formate band intensity drops immediately right after the potential step, while the CO_{ad} signal develops slowly with time. Both facts indicate that formate is not the reactive intermediate for formic acid dehydration to CO.

Key words: Mechanism for formic acid dehydration, Formate intermediate, CO pathway, Pt electrode, Infrared spectroscopic studies under attenuated total reflection configuration

I. INTRODUCTION

The electrocatalytic oxidation of formic acid (HCOOH) on Pt and Pt-based alloys has long been the research focus in the field of electrochemistry [1−8]. It is a model system for studying electrocatalytic oxidation of small organic molecules due to its simple molecular structure. On the other hand, HCOOH is of great potential as fuel for low temperature fuel cells. Extensive studies have also been carried out aiming at understanding formic acid oxidation mechanism and developing highly efficient catalysts for this process [4, 6]. It is well accepted that this reaction proceeds via dual path mechanisms with a direct and an indirect pathway [3, 5]:

$$\mathrm{HCOOH} \rightarrow \text{Active intermediate} \rightarrow \mathrm{CO_2}$$
$$\mathrm{HCOOH} \rightarrow \text{Poison intermediate } (\mathrm{CO_{ad}}) \dashrightarrow \mathrm{CO_2}$$

However, the detailed mechanism for the direct and indirect pathway with respect to the oxidation of formic acid at Pt electrode is still under hot debate [9]. During formic acid oxidation at Pt electrode, linearly, bridge and hollow site adsorbed CO (CO_L, CO_B, and CO_H) and bridge-bonded formate ($HCOO_b$) have been well confirmed by electrochemical *in-situ* infrared spectroscopic studies under attenuated total reflection configuration (EC-ATR-FTIRS) [9−15]. It is still under hot discussion on role of $HCOO_b$ in HCOOH oxidation [9, 15−20]. Several groups concluded that $HCOO_b$ is the reactive intermediate in the main pathway responsible for the majority current for HCOOH oxidation, however, they proposed three distinct mechanisms for the formate pathway with either first or second order reaction kinetics [15, 17, 18]. In contrast, based on the lacking of defined relationship between formate coverage and formic acid oxidation current at both Pt film and Pt(111) electrodes [19−21], we concluded that bridge-bonded formate is not the reactive intermediate for the direct pathway in formic acid oxidation.

As for the indirect pathway for formic acid oxidation, it is suggested that it proceeds via the initial dehydration of HCOOH to CO_{ad}, which is then, oxidized to CO_2 [5, 22, 23]. Our systematic studies on the concentration, temperature and potential effects on formic acid oxidation reveal that the contribution of the current from CO pathway to the total current for formic acid oxidation is negligible [16]. And it is well confirmed that the formed CO_{ad} will accumulate on the catalysts surface which will finally poison the electrocatalytic oxidation of HCOOH. Hence, knowledge on how CO_{ad} is formed from HCOOH under catalytic conditions will be of great help in designing improved catalysts to mitigate or even eliminate the CO_{ad} poisoning problem. So far, only few studies discussed how CO_{ad} is formed from HCOOH under catalytic conditions [17, 18, 24−28]. Based on the linear relationship between CO_{ad} formation rate and the change in the band inten-

*Author to whom correspondence should be addressed. E-mail: yachen@ustc.edu.cn

sity of bridge-bonded formate from an electrochemical *in-situ* ATR-FTIR spectroscopic study, Cuesta *et al.* suggested that $HCOO_b$ is also the reactive intermediate for CO_{ad} formation from formic acid dehydration [28]. In this work, we will demonstrate that using the same ATR-FTIRS technique, such a relationship cannot be obtained at all. Possible origins for the discrepancy of the experimental data and the role for $HCOO_b$ in HCOOH dehydration to CO_{ad} will be discussed.

II. EXPERIMENTS

The working electrode used is a 50 nm thick Pt film (roughness factor≈7) deposited onto the flat plane of a hemi-cylindrical Si prism [29, 30]. A Pt foil and a reversible hydrogen electrode (RHE) are used as the counter electrode (CE) and the reference electrode (RE), respectively. Two kinds of spectroelectrochemical cells *i.e.*, a thermostatic cell and a the flow cell, were employed for electrochemical *in-situ* ATR-FTIRS measurements.

The structures of thermostatic cell and the flow cell are described in Refs.[16, 19]. In brief, the flow cell consists of a circular Kel-F plate with openings for inlet and outlet capillaries. The working electrode (WE) is Pt thin film which is coated on the flat plane of the hemi-cylindrical silicon prism. The prism together with the WE is pressed against the Kel-F plate through a circular gasket and a Cu foil current collector. The volume of the flow cell is ca. 18 μL and the flow rate of electrolyte is ca. 250 μL/s, which makes the *in situ* ATR-FTIRS studies under continuous and well defined flow conditions. During measurement with flow cell, the electrolyte can be easily switched to supplying bottles containing electrolyte of different composition.

The thermostatic cell is modified from a conventional three electrode glass cell. In the thermostatic cell, the cell temperature is controlled by circulating water through its glass jacket, which is connected to a thermal bath. In order to make sure that CO_{ad} formation rate is not too fast so that we can follow the relation of CO_{ad} formation rate to the change of formate band intensity in detail, cell temperature is kept at 5 °C in the potential step experiments. A potentiostat (PAR 273A, Ametek, USA) is used to control the electrode potential, all potentials are quoted against the RHE.

Millipore Milli-Q water, ultrapure perchloric acid (Suprapure, Sigma-Aldrich), and formic acid (for analysis, Fluka) were used to prepare the solutions. Supporting electrolyte used in this study was 0.1 mol/L $HClO_4$. The concentration of formic acid solution used in this study was 0.1 or 0.02 mol/L. During the measurement, the electrolyte is constantly purged with N_2 (5N, Nanjing Special Gas Corp.). Before the measurements, continuous potential cycles in the potential region from 0.05 V to 1.3 V at a scan rate of 0.05 V/s in 0.1 mol/L $HClO_4$ were carried out to clean Pt thin film electrode until its cyclic voltammogram (CV) becomes reproducible.

In the solution switch experiment in the flow cell, electrode potential is first held at 0.4 V in 0.1 mol/L $HClO_4$, then it is switched to 0.1 mol/L $HClO_4$+0.02 mol/L HCOOH, and the reaction current, CO_{ad} and $HCOO_b$ band intensity are recorded. In order to follow the CO_{ad} formation rate and its relation to the change of formate coverage, potential step experiment was carried out in the stationary thermostatic cell and choronoamperometric measurements at constant potential when switching the electrolyte from HCOOH free to HCOOH containing solutions have been carried out.

In-situ IR measurements were carried out with a Varian FTS 7000e infrared spectrometer equipped with a mercury cadmium telluride (MCT) detector cooled by liquid nitrogen. All the spectra were obtained with a resolution of 4 cm^{-1}. In order to follow the spectral change, the spectrum integration time was 1.0 s for the solution switch experiment in the flow cell and 0.3 s for the potential step experiment in the stationary cell, respectively. All spectra were shown in absorbance, *i.e.* $\lg(R_0/R)$, where R_0 is the reflectance of the background spectrum recorded at the same potential on clean Pt electrode in the supporting electrolyte without formic acid. This data processing results in spectra with peaks pointing up arising from the gain of absorption in R with respect to R_0, and peaks pointing down, to the loss of absorption in R compared to R_0.

III. RESULTS AND DISCUSSION

Figure 1(a) shows CV for the Pt film electrode in 0.1 mol/L $HClO_4$. It displays well defined feature for the under potential deposition (UPD) of H and the oxidative removal of UPD-H atoms in the potential region from 0.05 V to 0.4 V, which is followed with a double layer region from 0.4 V to 0.7 V and region for Pt-OH and Pt-O_x formation at E>0.75 V and the corresponding reduction wave in the negative-going potential scan. Such CV reproduces well the features for Pt film as reported in Ref.[31]. On the other hand, the CV recorded in 0.1 mol/L $HClO_4$+0.1 mol/L HCOOH (Fig.1(b)) also displays characteristic features for formic acid oxidation as reported in Refs.[13, 16]. As can be seen, in the positive-going scan, currents are much lower than in the negative-going one, due to the formation of CO at low potentials, which blocks the electrode surface for the direct oxidation. At E>0.75 V, CO is readily oxidized and the surface is free of CO while the formation of Pt-OH and Pt-O_x inhibits the oxidation of formic acid. In the return scan, the amount of accumulated CO is lower and currents are higher. The CVs recorded in the stationary cell is nearly the same as that recorded in the flow cell. Both CVs suggest that the Pt film prepared is of good quality and the cell system is clean.

Figure 2 shows sequences of IR spectra recorded

DOI:10.1063/1674-0068/26/04/471-476

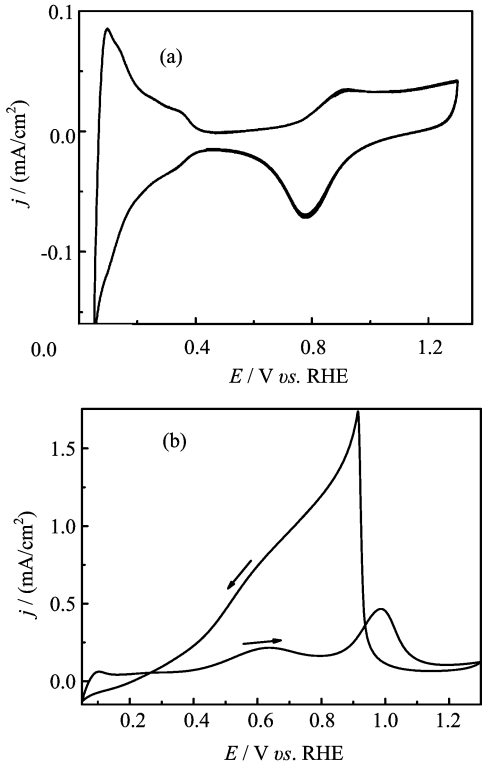

FIG. 1 (a) Cyclic voltammogram for a Pt film electrode recorded in 0.1 mol/L $HClO_4$ before the addition of HCOOH. (b) Cyclic voltammogram for the same Pt electrode film recorded in 0.1 mol/L HCOOH+0.1 mol/L $HClO_4$ at a potential scan rate of 50 mV/s.

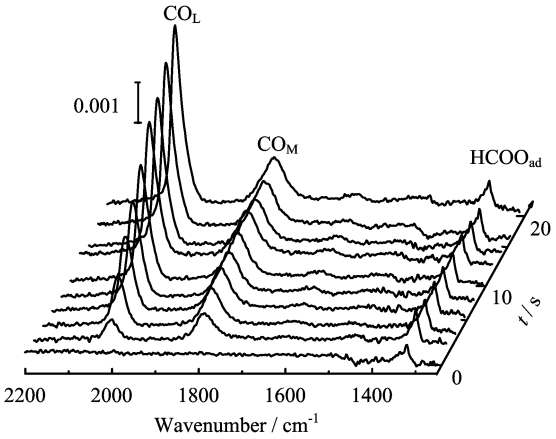

FIG. 2 Sequences of selected IR spectra at Pt surface recorded in the first 20 s after the electrolyte exchange from 0.1 mol/L $HClO_4$ to 0.1 mol/L $HClO_4$+0.02 mol/L HCOOH at 0.4 V. The spectral time resolution is 1 s.

within the first 20 s after switching the electrolyte from 0.1 mol/L $HClO_4$ to 0.1 mol/L $HClO_4$+ 0.02 mol/L HCOOH at 0.4 V. The bands in the region from 1700 cm^{-1} to 2100 cm^{-1} come from adsorbed CO species, *i.e.*, on on-top CO_L (2000−2065 cm^{-1}) and on bridge- or multifold sites (CO_M, 1790−1880 cm^{-1}). The spectra show a clear increase in band intensity and peak frequency of the $CO_{L,M}$ band with time, reflecting an increasing CO_{ad} coverage. And in the low frequency region, a characteristic peak at 1320 cm^{-1} from bridge-bonded formate appears [3, 7, 17], whose band intensity increases quickly and reaches maximum at ca. 1 s after solution switch.

Figure 3 gives the current density transients and the integrated band intensity of the CO_L and CO_M species during formic acid adsorption/oxidation at 0.4 V as a function of time. From careful calibration [19, 32], we found that there is a linear relationship between CO_{ad} coverage and the integrated band intensity of CO_L and CO_B in different coverage regime. Since at E<0.5 V at room temperature, CO_{ad} oxidation is negligibly slow [16, 33], hence CO_{ad} formation rate just equals to $d\theta_{CO}/dt$, which can be easily derived from such linear relationship and is also plotted in Fig.3(c). From Fig.3(c), it is seen that CO_{ad} formation rate decreases with reaction time. And there is no clear relationship between CO_{ad} formation rate and formate surface coverage, *e.g.*, CO_{ad} formation rate is the highest when formate surface coverage is zero, after ca. 1 s formate converage reaches maximum, while CO_{ad} formation rate continues its decay with time up to ca. 30 s. In a word, no linear relationship between formate band intensity and CO_{ad} formation rate is observed, as in contrast to previous report by Cuesta *et al.* [27].

In order to further confirm whether there is any defined relationship between CO_{ad} formation rate and $HCOO_b$ surface coverage, we have also carried out potential step measurements. Figure 4 shows a series of time-resolved IR spectra recorded during potential step from 0.75 V to 0.35 V in 0.1 mol/L $HClO_4$+0.1 mol/L HCOOH at 5 °C. Only the spectra recorded within the first 3 s before and after the potential step are shown for clarity. From the figure, it is seen that at 0.75 V, only the symmetric O−C−O stretching of $HCOO_b$ is observed. Immediately after stepping to 0.35 V, formate band intensity drops to a smaller value and then it remains constant with time. On the other hand, band for CO_L and CO_M in the region from 1700 cm^{-1} to 2100 cm^{-1} appears, whose band intensity increases with time, at a much slower rate than the drop for the formate band. This is seen more clearly from the band intensity-time profiles (Fig.5(b)) derived by integrating the IR bands of the CO_L , CO_M and $HCOO_{ad}$ species recorded during potential step from 0.75 V to 0.35 V. Similar phenomena have also been observed when stepping the electrode potential from 0.75 V to 0.4 V and 0.45 V.

Again, since CO_{ad} oxidation is negligibly slow at E<0.5 V and 5 °C, the CO_{ad} band intensity-time profiles just give the rate for CO_{ad} formation from HCOOH decomposition under such circumstance. The ill correlation between the change of formate and CO_{ad} band intensity from both flow cell measurements under con-

DOI:10.1063/1674-0068/26/04/471-476

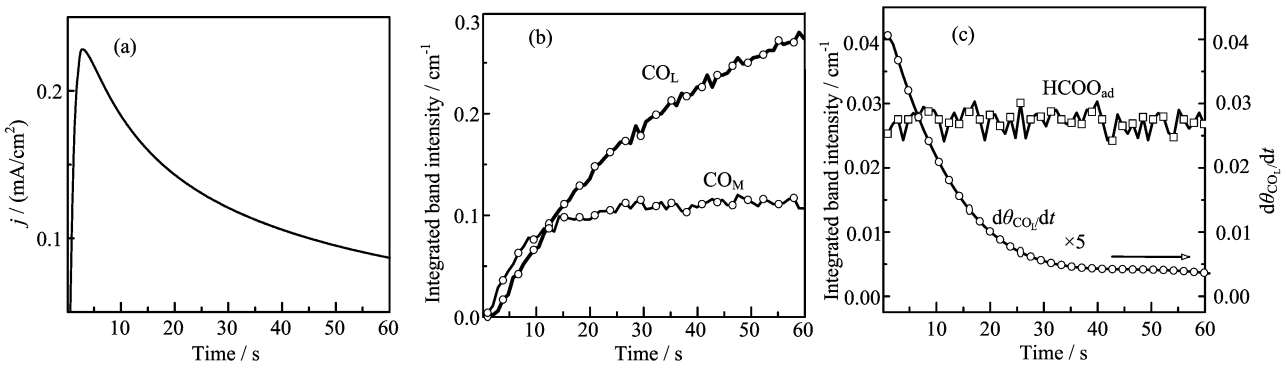

FIG. 3 (a) Current-density transient. (b) Integrated band intensity of CO_L and CO_M as a function of time after changing from 0.1 mol/L $HClO_4$ to 0.1 mol/L $HClO_4$+0.02 mol/L HCOOH at a constant potential of 0.4 V. (c) Integrated $HCOO_{ad}$ band intensity as a function of time after changing from 0.1 mol/L $HClO_4$ to 0.1 mol/L $HClO_4$+0.02 mol/L HCOOH at a constant potential of 0.4 V, and time dependence of $d\theta_{CO_L}/dt$ is also plotted. The curves are derived from raw data given in Fig.2.

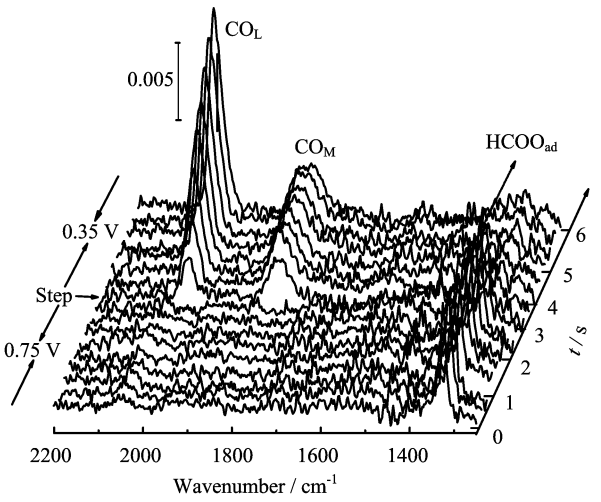

FIG. 4 IR spectra at Pt surface recorded within 6 s during the potential step from 0.75 V to 0.35 V in 0.1 mol/L $HClO_4$+0.1 mol/L HCOOH at 5 °C. The spectral time resolution was 0.3 s.

stant electrode potential and during potential step measurements in stationary cell reveals that formate should not be the reactive intermediate for HCOOH dehydration to CO_{ad}. In fact, our recent study at Pt(111) electrode shows that formate adsorption/desorption follows Frumkin-type adsorption isotherm and the intrinsic rate for formate adsorption/desorption is very fast [34]. In our present experiments, the adsorption of formate is so fast that its intensity reaches equilibrium within the time resolution used under present conditions. The abrupt drop when stepping from 0.75 V to 0.35 V is probably due to formate desorption induced by the change of excess charges at the electrode/electrolyte interface, it is not consumed through decomposition to CO_{ad} at all.

In our previous experiments in solution with 0.1 mol/L DCOOH, we have also observed that after switching from the electrolyte to DCOOH solution the rate of CO_{ad} formation decreases rapidly in the first 5 s, while the band intensity of $DCOO_{ad}$ increases quickly to its maximum and keeps stable in the subsequent potentiostatic measurement [20]. The decrease of the rate for formic acid dehydration to CO_{ad} formation with increase in formate coverage in the solution switch experiments indicates that formate is not the intermediate for CO_{ad} formation, instead it indicates that formate adsorbate may inhibit the dehydration of formic acid to CO_{ad} through competing for the empty sites. Furthermore, from solution switch experiments at constant potentials with $E \leq 0.2$ V, we found that no formate is formed at Pt surface, however, formic acid decomposition to CO_{ad} occurs and its rate increases with electrode potential from 0.05 V to 0.2 V. Similar phenomena have also been observed on the series of platinum single-crystal electrodes [18, 35, 36]. All these facts further support that formate is not the reactive intermediates for formic acid dehydration to CO_{ad}.

Interestingly, from a recent ATR-FTIRS study in a stationary cell, Cuesta *et al.* observed that when holding the electrode potential at constant potential E=0.355 V, both CO_{ad} and formate band signal first increases within first few seconds after addition of formic acid into the solution of adsorption. By quantivative analysis, they found that CO_{ad} formation rate first increases with time then it decrease again, this trend is just exactly the same as the change in formate band intensity with time, *i.e.*, $d\theta_{CO}/dt \propto \theta_{formate}$. From which, they concluded that CO_{ad} is mainly generated from $HCOOH_{ad}$ through $HCOO_{ad}$ intermediate [28]. In contrast, in our study, we never observe such a linear relationship for $d\theta_{CO}/dt \propto \theta_{formate}$, in fact we found that there is $d\theta_{CO}/dt \propto (1 - \theta_{CO} - \theta_{formate})^2$. This indicates that CO_{ad} formation needs two free sites, detailed discussion on the mechanism for CO_{ad} formation will be given in another work.

The different experimental behavior between our lab

DOI:10.1063/1674-0068/26/04/471-476

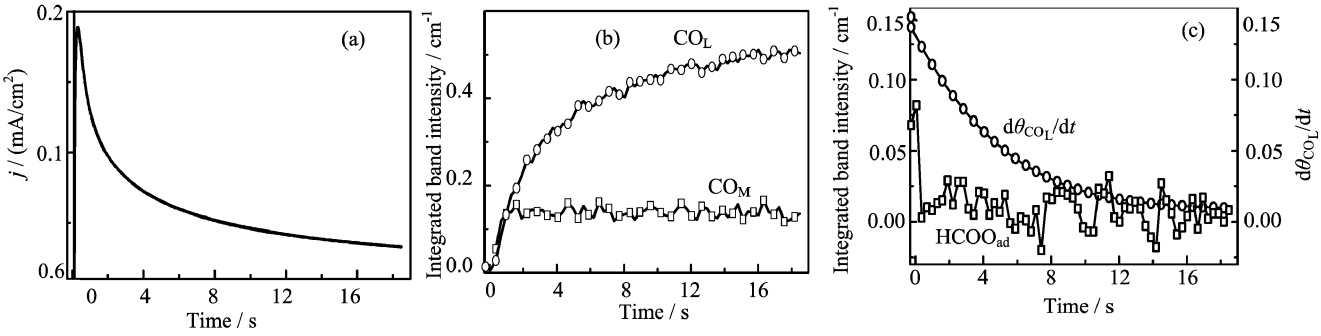

FIG. 5 (a) Current-density transient. (b) Integrated band intensity of $CO_L$and CO_M as a function of time after potential step from 0.75 V to 0.35 V. (c) Integrated band intensity of $HCOO_{ad}$ as a function of time after potential step from 0.75 V to 0.35 V, and time dependence of $d\theta_{CO_L}/dt$ is also plotted.

and that from Cuesta's can be easily understood by the mass transport effect in Cuesta's experiments [27]. In order to observe the formation of $HCOO_{ad}$ and CO_{ad} in the first few seconds, Cuesta *et al.* employed a micropipette to add the concentrated HCOOH into the unstirred solution until the uniform concentration was reached. Within the first few seconds, the rates for both CO_{ad} formation and $HCOO_{ad}$ adsorption depend on the amount of HCOOH molecules reaching the surface, such a phenomenon only indicates that these processes within first few seconds are mass transport limited, it cannot be simply taken as $HCOO_{ad}$ is the intermediate for CO_{ad} formation. In fact, from the data sets obtained from the same group, it is found that the linear relationship of $d\theta_{CO}/dt \propto \theta_{formate}$ only applies for the data points within the first few second right after the injection of HCOOH. At longer time, when formic acid surface concentration reaches that of its bulk concentration, such linear behavior does not exist anymore as similar to the present observation. Our study indicates that when one wants to deduce reaction mechanism based on the kinetic data measured by spectroelectrochemical means, one should be very careful that whether the data are partially distorted by mass transport effect.

IV. CONCLUSION

In-situ ATR-FTIRS combined with solution exchange and potential-step chronoamperometry technique have been employed to clarify whether $HCOO_{ad}$ is the reactive intermediate for formic acid dehydration to CO_{ad} at Pt electrode. In the solution exchange experiment at constant potential, we found that the CO_{ad} formation rate decreases, while the $HCOO_{ad}$ intensity reaches equilibrium within first 1 s after solution switch. In the potential step experiment from 0.75 V to 0.35 V, CO_{ad} formation rate is also found to decrease with time, while the $HCOO_{ad}$ band intensity drops abruptly upon the potential step. Both sets of experiment data indicate that formate is not the reactive intermediate for formic acid dehydration to CO. Knowledge on the mechanism of how CO_{ad} is formed from HCOOH molecules at Pt electrode will be of great help to design improved catalysts against the CO poisoning problems in direct formic acid fuel cells. Unfortunately, so far there is no solid experimental evidence telling how CO_{ad} is formed from HCOOH molecules at Pt electrode. We have carried out macroscopic kinetic simulation on the relationship for CO_{ad} formation rate and empty sites, detailed results will be given elsewhere.

V. ACKNOWLEDGMENTS

This work was supported by the National Natural Science Foundation of China (No.21273215) and the National Key Basic Program of China (No.2010CB923302).

[1] A. Hamnett, *Accomplishments and Challenges, Interfacial Electrochemistry*, New York: Marcel Dekker Inc., 843 (1999).
[2] M. W. Breiter, J. Electroanal. Chem. **14**, 407 (1967).
[3] A. Capon and R. Parsons, J. Electroanal. Chem. **45**, 205 (1973).
[4] T. D. Jarvi and E. M. Stuve, *Electrocatalysis*, New York: Wiley-VCH, 75 (1998).
[5] S. G. Sun, *Studying Electrocatalytic Oxidation of Small Organic Molecules With In-Situ Infrared Spectroscopy*, in: J. Lipkowski, P. N. Ross, Eds. *Electrocatalysis*, New York: Wiley-VCH, 243 (1998).
[6] B. Beden, J. M. Leger, and C. Lamy, *Modern Aspects of Electrochemistry*, New York: Plenum, 97 (1992).
[7] E. Herrero and J. Feliu, *Encyclopedia Electrochemistry Interfacial Kinetics and Mass Transport*, Weinheim, Germany: Wiley-VCH, 443 (2003).
[8] P. Waszczuk, A. Crown, S. Mitrovski, and A. Wieckowski, *Electrocatalysis, Handbook of Fuel Cells*, Chichester, the UK: John Wiley & Sons, 635 (2003).
[9] G. Samjeske and M. Osawa, Angew. Chem. Int. Ed. **44**, 5694 (2005).

DOI:10.1063/1674-0068/26/04/471-476

[10] A. Kutschker and W. Vielstich, Electrochim. Acta **8**, 985 (1963).
[11] R. Gomez, J. M. Orts, J. M. Feliu, J. Clavilier, and L. H. Klein, J. Electroanal. Chem. **432**, 1 (1997).
[12] G. Samjeske, A. Miki, S. Ye, A. Yamakata, Y. Mukouyama, H. Okamoto, and M. Osawa, J. Phys. Chem. B **109**, 23509 (2005).
[13] G. Samjeske, A. Miki, S. Ye, and M. Osawa, J. Phys. Chem. B **110**, 16559 (2006).
[14] Y. Mukouyama, M. Kikuchi, G. Samjeske, M. Osawa, and H. Okamoto, J. Phys. Chem. B **110**, 11912 (2006).
[15] M. Osawa, K. I. Komatsu, G. Samjeske, T. Uchida, T. Ikeshoji, A. Cuesta, and C. Gutierrez, Angew. Chem. Int. Ed. **50**, 1159 (2011).
[16] Y. X. Chen, S. Ye, M. Heinen, Z. Jusys, M. Osawa, and R. J. Behm, J. Phys. Chem. B **110**, 9534 (2006).
[17] A. Cuesta, G. Cabello, M. Osawa, and C. Gutierrez, Acs Catalysis **2**, 728 (2012).
[18] V. Grozovski, F. J. Vidal-Iglesias, and E. Herrero, J. M. Feliu, ChemPhysChem **12**, 1641 (2011).
[19] Y. X. Chen, M. Heinen, Z. Jusys, and R. J. Behm, Angew. Chem. Int. Ed. **45**, 981 (2006).
[20] Y. X. Chen, M. Heinen, Z. Jusys, and R. J. Behm, Langmuir **22**, 10399 (2006).
[21] J. Xu, D. F. Yuan, F. Yang, D. Mei, Z. B. Zhang, and Y. X. Chen, Phys. Chem. Chem. Phys. **15**, 4367 (2013).
[22] V. Grozovski, V. Climent, E. Herrero, and J. M. Feliu, Phys. Chem. Chem. Phys. **12**, 8822 (2010).
[23] O. Wolter, J. Willsau, and J. Heitbaum, J. Electrochem. Soc. **132**, 1635 (1985).
[24] M. D. Macia, E. Herrero, J. M. Feliu, and A. Aldaz, J. Electroanal. Chem. **500**, 498 (2001).
[25] M. D. Macia, E. Herrero, J. M. Feliu, and A. Aldaz, Electrochem. Commun. **1**, 87 (1999).
[26] A. Wieckowski and J. Sobkowski, J. Electroanal. Chem. **63**, 365 (1975).
[27] A. Cuesta, G. Cabello, C. Gutierrez, and M. Osawa, Phys. Chem. Chem. Phys. **13**, 20091 (2011).
[28] A. Cuesta, M. Escudero, B. Lanova, and H. Baltruschat, Langmuir **25**, 6500 (2009).
[29] A. Miki, S. Ye, and M. Osawa, Chem. Commun. **14**, 1500 (2002).
[30] A. Miki, S. Ye, T. Senzaki, and M. Osawa, J. Electroanal. Chem. **563**, 23 (2004).
[31] Y. X. Chen, A. Miki, S. Ye, H. Sakai, and M. Osawa, J. Am. Chem. Soc. **125**, 3680 (2003).
[32] L. W. Liao, S. X. Liu, Q. Tao, B. Geng, P. Zhang, C. M. Wang, Y. X. Chen, and S. Ye, J. Electroanal. Chem. **650**, 233 (2011).
[33] Y. X. Chen, M. Heinen, Z. Jusys, and R. J. Behm, ChemPhysChem **8**, 380 (2007).
[34] J. Xu, C. H. Lin, D. Mei, Z. B. Zhang, D. F. Yuan, and Y. X. Chen, Chin. J. Chem. Phys **26**, 191 (2013).
[35] V. Grozovski, V. Climent, E. Herrero, and J. M. Feliu, ChemPhysChem **10**, 1922 (2009).

DOI:10.1063/1674-0068/26/04/471-476